Supplementary Materials for:

Evaluating the Impacts of ACP Management on the Energy Performance of Hydrothermal Liquefaction via Nutrient Recovery

Sarah K. Bauer [1,†], Fangwei Cheng [2,†] and Lisa M. Colosi [2,*]

[1] Department of Civil and Environmental Engineering, Rowan University, 201 Mullica Hill Road, Glassboro, NJ 08028, USA; bauers@rowan.edu
[2] Department of Engineering Systems and Environment, University of Virginia, 351 McCormick Road, Charlottesville, VA 22904, USA; fc4uk@virginia.edu
† These authors contributed equally to this paper.
* Correspondence: lmc6b@virginia.edu; Tel.: +1-434-924-7962; Fax: +1-434-982-2951

Table of Contents

1.0. Modeling Considerations for the Recovery of Nutrients from Post-HTL ACP

It is of interest to recover nitrogen (N) and phosphorus (P) via chemical precipitation from post-HTL ACP in the form of ammonium (NH_4–N) and orthophosphate (PO_4–P). Thus, it is important to understand the aquatic chemistry of these substances, specifically the speciation of N and P as a function of pH. Figure S1 shows the speciation of ammonia (NH_3) between ionized NH_4^+ and free NH_3, as well as the orthophosphate (OP) species over a pH range of 0–14.

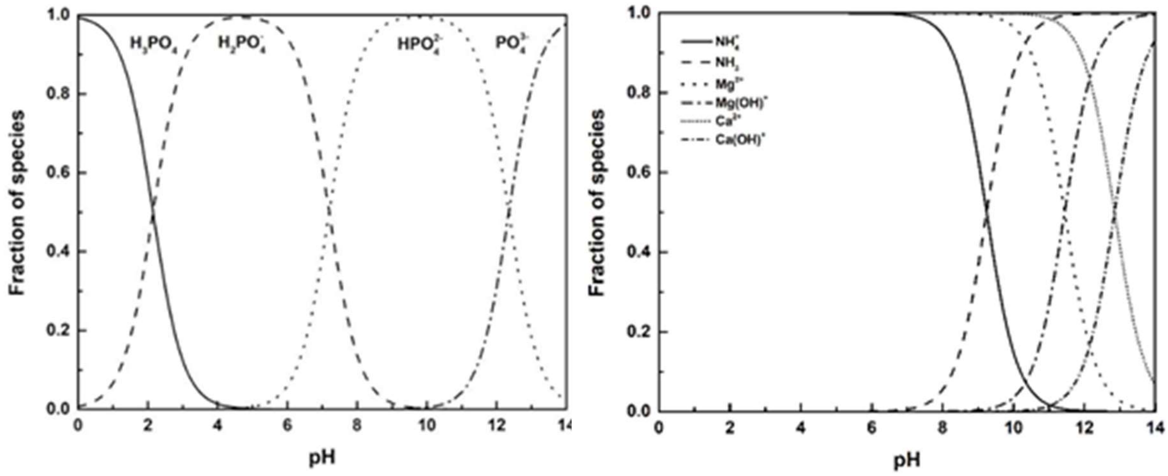

(**a**) (**b**)

Figure S1. pH dependence of (**a**) OP and (**b**) ammonia, magnesium, and calcium speciation at 25 °C. The speciation of ammonia between ionized NH_4^+ and free NH_3, as well as the OP species (i.e., H_3PO_4, $H_2PO_4^-$, HPO_4^{2-}, and PO_4^{3-}) is pH-dependent.

The chemical modeling software Visual MINTEQ Version 3.1, originally developed by the U.S. EPA, was used to determine an optimal pH value for each post-HTL ACP for maximum N and P recovery as struvite [1].

2.0. Modeling Results for the Theoretical Recovery of Nutrients from Post-HTL ACP

Visual MINTEQ modeling was used to determine the theoretical recovery of dissolved nutrients from each of the ACPs in the form of struvite. Tables S1 through S7 present the model results for each ACP individually for a wide range of pH values, starting at the initial pH of each ACP. The model was programmed separately for each ACP with various water quality input data. The data in columns 3–6 are based on outputs from the model, whereas the values in column 2 are based on laboratory results. Column 2 quantifies the volume of sodium hydroxide (NaOH) required to raise the pH of the ACPs to a given value. The model was varied for each ACP based on two variables: pH and concentration of Mg^{2+}, in order to evaluate the precipitation of struvite. The value of pH was increased at a rate of 0.5 from the starting value of each ACP to pH 14. Mg^{2+} was increased from the initial concentration in each ACP by 5 mg/L for 500 steps using the "Multi Problem/Sweep" function of the model.

Table S1. Theoretical recovery of nutrients via the precipitation of struvite from post-HTL dairy manure ACP at a pH range of 4.4 to 14. Initial PO_4^{3-} = 1.27 mM; Initial NH_4^+ = 22.5 mM.

pH	NaOH Consumed (mM)	$MgCl_2$ Consumed (mM)	Recovered Struvite (mM)	Recovered OP (mM)	Recovered NH_4^+/NH_3 (mM)	Principal Dissolved Complexes of Theoretically Recoverable Nutrients
4.4	-	0	0	0	0	NH_4^+ (100%); $H_2PO_4^-$ (90%)
4.5	0.40	0	0	0	0	NH_4^+ (100%); $H_2PO_4^-$ (90%)
5.0	0.55	0	0	0	0	NH_4^+ (100%); $H_2PO_4^-$ (89%)
5.5	0.69	0	0	1.03	0	NH_4^+ (100%); $H_2PO_4^-$ (87%)
6.0	0.83	0	0	1.25	0	NH_4^+ (100%); $H_2PO_4^-$ (78%); HPO_4^{2-} (8%)
6.5	0.98	0	0	1.26	0	NH_4^+ (100%); $H_2PO_4^-$ (57%); HPO_4^{2-} (20%)
7.0	1.12	0	0	1.26	0	NH_4^+ (99%); $H_2PO_4^-$ (31%); HPO_4^{2-} (34%)
7.5	1.27	0	0	1.26	0	NH_4^+ (98); $H_2PO_4^-$ (12%); HPO_4^{2-} (43%)
8.0	**1.41**	**0**	**0**	**1.27**	**0**	**NH_4^+ (95%); NH_3 (aq) (5%)**
8.5	1.55	0	0	1.27	0	NH_4^+ (87%); NH_3 (aq) (13%)
9.0	1.70	0	0	1.27	0	NH_4^+ (67%); NH_3 (aq) (32%)
9.5	1.84	0	0	1.27	0	NH_4^+ (40%); NH_3 (aq) (60%)
10	1.99	0	0	1.27	0	NH_4^+ (17%); NH_3 (aq) (82%)
10.5	2.13	0	0	1.27	0	NH_4^+ (6%); NH_3 (aq) (93%)
11	2.27	0	0	1.27	0	NH_3 (aq) (97%)
11.5	2.42	0	0	1.27	0	NH_3 (aq) (99%)
12	2.56	0	0	1.27	0	NH_3 (aq) (99%)
12.5	2.70	0	0	1.27	0	NH_3 (aq) (99%)
13	2.85	0	0	1.27	0	NH_3 (aq) (100%)
13.5	2.99	0	0	1.03	0	NH_3 (aq) (100%)
14	3.14	0	0	1.25	0	NH_3 (aq) (100%)

Table S2. Theoretical recovery of nutrients via the precipitation of struvite from post-HTL pre-digested sludge ACP at a pH range of 8.4 to 14. Optimal pH for nutrient recovery from pre-digested sludge ACP is 10.5. Initial PO_4^{3-} = 3.6 mM; Initial NH_4^+ = 69.6 mM.

pH	NaOH Consumed (mM)	$MgCl_2$ Consumed (mM)	Recovered Struvite (mM)	Recovered OP (mM)	Recovered NH_4^+/NH_3 (mM)	Principal Dissolved Complexes of Theoretically Recoverable Nutrients
8.4	-	3.29	3.12	3.43	3.12	NH_4^+ (83%); NH_3 (aq) (16%); HPO_4^{2-} (89%)
8.5	0.01	3.29	3.15	3.45	3.15	NH_4^+ (86%); NH_3 (aq) (13%); HPO_4^{2-} (90%)
9.0	0.10	3.29	3.23	3.53	3.23	NH_4^+ (68%); NH_3 (aq) (32%); HPO_4^{2-} (92%)
9.5	0.40	3.29	3.26	3.57	3.26	NH_4^+ (40%); NH_3 (aq) (60%); HPO_4^{2-} (92%)
10	0.70	3.29	3.27	3.58	3.27	NH_4^+ (17%); NH_3 (aq) (83%); HPO_4^{2-} (91%)
10.5	**1.00**	**3.29**	**3.28**	**3.59**	**3.28**	**NH_4^+ (6%); NH_3 (aq) (94%); HPO_4^{2-} (87%)**
11	1.30	3.29	3.28	3.58	3.28	NH_3 (aq) (98%); HPO_4^{2-} (80%); PO_4^{3-} (6%)
11.5	1.60	3.29	3.25	3.56	3.25	NH_3 (aq) (98%); HPO_4^{2-} (64%); PO_4^{3-} (15%)
12	1.90	3.29	2.69	2.99	2.69	NH_3 (aq) (99%); HPO_4^{2-} (49%); PO_4^{3-} (40%)
12.5	2.20	3.29	0	0.30	0	NH_3 (aq) (99%); HPO_4^{2-} (21%); PO_4^{3-} (72%)
13	2.50	3.29	0	0.30	0	NH_3 (aq) (100%); HPO_4^{2-} (6%); PO_4^{3-} (88%)
13.5	2.79	3.29	0	0.30	0	NH_3 (aq) (100%); PO_4^{3-} (95%)
14	3.09	3.29	0	0.30	0	NH_3 (aq) (100%); PO_4^{3-} (97%)

Table S3. Theoretical recovery of nutrients via the precipitation of struvite from post-HTL digested sludge ACP at a pH range of 8.6 to 14. Optimal pH for nutrient recovery from digested sludge ACP is 10.5. Initial PO_4^{3-} = 0.99 mM; Initial NH_4^+ = 149.9 mM.

pH	NaOH Consumed (mM)	$MgCl_2$ Consumed (mM)	Recovered Struvite (mM)	Recovered OP (mM)	Recovered NH_4^+/NH_3 (mM)	Principal Dissolved Complexes of Theoretically Recoverable Nutrients
8.6	-	0.41	0.390	0.878	0.390	NH_4^+ (87%); NH_3 (aq) (12%); HPO_4^{2-} (93%)
9.0	0.16	0.41	0.438	0.928	0.438	NH_4^+ (68%); NH_3 (aq) (31%); HPO_4^{2-} (92%)
9.5	0.39	0.41	0.468	0.958	0.468	NH_4^+ (40%); NH_3 (aq) (60%); HPO_4^{2-} (93%)
10	0.94	0.41	0.479	0.970	0.479	NH_4^+ (17%); NH_3 (aq) (83%); HPO_4^{2-} (91%)
10.5	**1.50**	**0.41**	**0.482**	**0.973**	**0.482**	**NH_4^+ (6%); NH_3 (aq) (94%); HPO_4^{2-} (88%)**
11	2.05	0.41	0.479	0.971	0.479	NH_3 (aq) (98%); HPO_4^{2-} (81%); PO_4^{3-} (6%)
11.5	2.60	0.41	0.467	0.958	0.467	NH_3 (aq) (98%); HPO_4^{2-} (66%); PO_4^{3-} (17%)
12	3.15	0.41	0.207	0.699	0.207	NH_3 (aq) (99%); HPO_4^{2-} (47%); PO_4^{3-} (41%)
12.5	3.70	0.41	0	0.491	0	NH_3 (aq) (99%); HPO_4^{2-} (22%); PO_4^{3-} (69%)
13	4.26	0.41	0	0.491	0	NH_3 (aq) (100%); HPO_4^{2-} (7%); PO_4^{3-} (87%)
13.5	4.81	0.41	0	0.492	0	NH_3 (aq) (100%); PO_4^{3-} (95%)
14	5.36	0.41	0	0.492	0	NH_3 (aq) (100%); PO_4^{3-} (97%)

Table S4. Theoretical recovery of nutrients via the precipitation of struvite from post-HTL brewing yeast ACP at a pH range of 8.3 to 14. Optimal pH for nutrient recovery from brewing yeast ACP is 10.5. Initial PO_4^{3-} = 24.3 mM; Initial NH_4^+ = 97.8 mM.

pH	NaOH Consumed (mM)	$MgCl_2$ Consumed (mM)	Recovered Struvite (mM)	Recovered OP (mM)	Recovered NH_4^+/NH_3 (mM)	Principal Dissolved Complexes of Theoretically Recoverable Nutrients
8.3	-	23.9	23.72	24.02	23.72	NH_4^+ (84%); NH_3 (aq) (15%); HPO_4^{2-} (83%)
8.5	0.06	23.9	23.78	24.08	23.78	NH_4^+ (87%); NH_3 (aq) (12%); HPO_4^{2-} (84%)
9.0	0.33	23.9	23.87	24.18	23.87	NH_4^+ (68%); NH_3 (aq) (31%); HPO_4^{2-} (86%)
9.5	0.60	23.9	23.92	24.22	23.92	NH_4^+ (42%); NH_3 (aq) (58%); HPO_4^{2-} (86%)
10	0.87	23.9	23.93	24.23	23.93	NH_4^+ (12%); NH_3 (aq) (81%); HPO_4^{2-} (85%)
10.5	**1.14**	**23.9**	**23.94**	**24.24**	**23.94**	**NH_4^+ (6%); NH_3 (aq) (94%); HPO_4^{2-} (82%)**
11	1.41	23.9	23.93	24.23	23.93	NH_3 (aq) (98%); HPO_4^{2-} (75%); PO_4^{3-} (7%)
11.5	1.68	23.9	23.90	24.22	23.90	NH_3 (aq) (98%); HPO_4^{2-} (59%); PO_4^{3-} (17%)
12	1.95	23.9	23.21	23.51	23.21	NH_3 (aq) (99%); HPO_4^{2-} (39%); PO_4^{3-} (38%)
12.5	2.23	23.9	0	0.30	0	NH_3 (aq) (99%); HPO_4^{2-} (14%); PO_4^{3-} (72%)
13	2.50	23.9	0	0.30	0	NH_3 (aq) (100%); HPO_4^{2-} (5%); PO_4^{3-} (83%)
13.5	2.77	23.9	0	0.30	0	NH_3 (aq) (100%); PO_4^{3-} (89%)
14	3.04	23.9	0	0.30	0	NH_3 (aq) (100%); PO_4^{3-} (92%)

Table S5. Theoretical recovery of nutrients via the precipitation of solids from post-HTL spent grains ACP at a pH range of 5.3 to 14. Optimal pH for nutrient recovery from spent grains ACP is 10.5. Initial PO43- = 11.4 mM; Initial NH4+ = 50.0 mM.

pH	NaOH Consumed (mM)	$MgCl_2$ Consumed (mM)	Recovered Struvite (mM)	Recovered OP (mM)	Recovered NH_4^+/NH_3 (mM)	Principal Dissolved Complexes of Theoretically Recoverable Nutrients
5.3	-	9.88	0	0	0	NH_4^+ (100%); $H_2PO_4^-$ (94%)
5.5	0.03	9.88	0	0	0	NH_4^+ (100%); $H_2PO_4^-$ (94%)
6.0	0.07	9.88	0	0	0	NH_4^+ (100%); $H_2PO_4^-$ (80%); HPO_4^{2-} (9%)
6.5	0.09	9.88	6.09	6.30	6.09	NH_4^+ (100%); $H_2PO_4^-$ (64%); HPO_4^{2-} (22%)
7.0	0.25	9.88	9.20	9.44	9.20	NH_4^+ (99%); $H_2PO_4^-$ (43%); HPO_4^{2-} (44%)
7.5	0.40	9.88	10.3	10.5	10.3	NH_4^+ (98%); $H_2PO_4^-$ (22%); HPO_4^{2-} (68%)
8.0	0.56	9.88	10.6	11.0	10.6	NH_4^+ (96%); $H_2PO_4^-$ (9%); HPO_4^{2-} (85%)
8.5	0.72	9.88	10.7	11.1	10.7	NH_4^+ (87%); NH_3 (aq) (13%); HPO_4^{2-} (93%)
9.0	0.88	9.88	10.8	11.2	10.9	NH_4^+ (68%); NH_3 (aq) (32%); HPO_4^{2-} (98%)
9.5	1.03	9.88	10.9	11.2	10.9	NH_4^+ (40%); NH_3 (aq) (60%); HPO_4^{2-} (99%)
10	1.19	9.88	11.0	11.2	11.0	NH_4^+ (17%); NH_3 (aq) (83%); HPO_4^{2-} (96%)
10.5	**1.35**	**9.88**	**11.1**	**11.3**	**11.1**	**NH_4^+ (6%); NH_3 (aq) (94%); HPO_4^{2-} (95%)**
11	1.50	9.88	11.0	11.2	11.0	NH_3 (aq) (98%); HPO_4^{2-} (89%); PO_4^{3-} (5%)
11.5	1.66	9.88	10.9	11.2	10.9	NH_3 (aq) (99%); HPO_4^{2-} (75%); PO_4^{3-} (14%)
12	1.82	9.88	10.3	10.5	10.3	NH_3 (aq) (99%); HPO_4^{2-} (55%); PO_4^{3-} (39%)
12.5	1.98	9.88	0	0.25	0	NH_3 (aq) (99%); HPO_4^{2-} (20%); PO_4^{3-} (79%)
13	2.13	9.88	0	0.25	0	NH_3 (aq) (100%); HPO_4^{2-} (6%); PO_4^{3-} (93%)
13.5	2.29	9.88	0	0.25	0	NH_3 (aq) (100%); PO_4^{3-} (98%)
14	2.45	9.88	0	0.25	0	NH_3 (aq) (100%); PO_4^{3-} (99%)

Table S6. Theoretical recovery of nutrients via the precipitation of solids from post-HTL white lees ACP at a pH range of 6.4 to 14. Optimal pH for nutrient recovery from white lees ACP is 9.0. Initial PO_4^{3-} = 1.1 mM; Initial NH_4^+ = 2.2 mM.

pH	NaOH Consumed (mM)	$MgCl_2$ Consumed (mM)	Recovered Struvite (mM)	Recovered OP (mM)	Recovered NH_4^+/NH_3 (mM)	Principal Dissolved Complexes of Theoretically Recoverable Nutrients
6.4	-	0	0	0.041	0	NH_4^+ (100%); $H_2PO_4^-$ (67%); HPO_4^{2-} (19%)
6.5	0.002	0	0	0.064	0	NH_4^+ (100%); $H_2PO_4^-$ (63%); HPO_4^{2-} (22%)
7.0	0.006	0	0	0.118	0	NH_4^+ (99%); $H_2PO_4^-$ (38%); HPO_4^{2-} (43%)
7.5	0.024	0	0	0.132	0	NH_4^+ (98%); $H_2PO_4^-$ (17%); HPO_4^{2-} (60%)
8.0	0.046	0	0	0.136	0	NH_4^+ (95%); $H_2PO_4^-$ (6%); HPO_4^{2-} (70%)
8.5	0.068	5.55	0.34	0.472	0.34	NH_4^+ (87%); NH_3 (aq) (13%); HPO_4^{2-} (51%)
9.0	**0.091**	**3.70**	**0.56**	**0.699**	**0.56**	**NH_4^+ (68%); NH_3 (aq) (32%); HPO_4^{2-} (57%)**
9.5	0.113	0.41	0.13	0.271	0.13	NH_4^+ (40%); NH_3 (aq) (60%); HPO_4^{2-} (71%)
10	0.135	0.21	0.09	0.227	0.09	NH_4^+ (18%); NH_3 (aq) (82%); HPO_4^{2-} (71%)
10.5	0.157	0	0	0.139	0	NH_4^+ (7%); NH_3 (aq) (93%); HPO_4^{2-} (70%)
11	0.179	0	0	0.139	0	NH_3 (aq) (98%); HPO_4^{2-} (64%); PO_4^{3-} (7%)
11.5	0.020	0	0	0.139	0	NH_3 (aq) (99%); HPO_4^{2-} (49%); PO_4^{3-} (17%)
12	0.224	0	0	0.139	0	NH_3 (aq) (99%); HPO_4^{2-} (29%); PO_4^{3-} (33%)
12.5	0.246	0	0	0.139	0	NH_3 (aq) (99%); HPO_4^{2-} (13%); PO_4^{3-} (49%)
13	0.268	0	0	0.139	0	NH_3 (aq) (100%); PO_4^{3-} (63%)
13.5	0.291	0	0	0.139	0	NH_3 (aq) (100%); PO_4^{3-} (77%)
14	0.313	0	0	0.139	0	NH_3 (aq) (100%); PO_4^{3-} (83%)

Table S7. Theoretical recovery of nutrients via the precipitation of solids from post-HTL red lees ACP at a pH range of 8.8 to 14. Optimal pH for nutrient recovery from red lees ACP is 10.5. Initial PO_4^{3-} = 22.2 mM; Initial NH_4^+ = 79.6 mM.

pH	NaOH Consumed (mM)	$MgCl_2$ Consumed (mM)	Recovered Struvite (mM)	Recovered OP (mM)	Recovered NH_4^+/NH_3 (mM)	Principal Dissolved Complexes of Theoretically Recoverable Nutrients
8.8	-	21.8	21.63	21.9	21.63	NH_4^+ (86%); NH_3 (aq) (14%); HPO_4^{2-} (61%)
9.0	0.16	21.8	21.68	22.0	21.68	NH_4^+ (70%); NH_3 (aq) (30%); HPO_4^{2-} (62%)
9.5	0.20	21.8	21.74	22.0	21.74	NH_4^+ (42%); NH_3 (aq) (58%); HPO_4^{2-} (61%)
10	0.66	21.8	21.76	22.0	21.76	NH_4^+ (19%); NH_3 (aq) (81%); HPO_4^{2-} (60%)
10.5	**1.12**	**21.8**	**21.77**	**22.1**	**21.77**	**NH_4^+ (7%); NH_3 (aq) (93%); HPO_4^{2-} (57%)**
11	1.58	21.8	21.76	22.0	21.76	NH_3 (aq) (98%); HPO_4^{2-} (49%); PO_4^{3-} (7%)
11.5	2.04	21.8	21.70	22.0	21.70	NH_3 (aq) (99%); HPO_4^{2-} (34%); PO_4^{3-} (15%)
12	2.50	21.8	19.08	19.4	19.08	NH_3 (aq) (99%); HPO_4^{2-} (19%); PO_4^{3-} (28%)
12.5	2.96	21.8	0	0.28	0	NH_3 (aq) (99%); HPO_4^{2-} (8%); PO_4^{3-} (43%)
13	3.42	21.8	0	0.28	0	NH_3 (aq) (100%); PO_4^{3-} (51%)
13.5	3.88	21.8	0	0.28	0	NH_3 (aq) (100%); PO_4^{3-} (60%)
14	4.34	21.8	0	0.28	0	NH_3 (aq) (100%); PO_4^{3-} (66%)

The results in Tables S1–S7 were used to determine the optimal pH value and Mg^{2+} addition to produce the maximum theoretical recovery of N and P from post-ACPs as struvite.

3.0. Energy Ratio Formulas and Parameterization

Life-cycle energy use for materials consumed and materials produced during the precipitation of nutrients from post-ACP as struvite were collected from the ecoinvent database, as accessed using SimaPro v.3 and/or adapted from Clarens et al. (2010) [2]. These data, presented in Table S8, were used to estimate energy return on investment [EROI] for ACP management and nutrient recovery.

Table S8. Summary of the life-cycle energy values of the various materials consumed and produced via the precipitation of nutrients from the post-HTL ACP of select organic waste feedstocks. Parameter values were taken from the ecoinvent database, as accessed using SimaPro v.3 and/or Clarens et al. (2010). MEOH = methanol.

	Material Type	Energy Cost (MJ/kg)
Materials Consumption	NaOH	46.6
	$MgCl_2$	4.7
	MEOH	38.0
	$FeSO_4$	1.95
Materials Production	MAP	13.5

Three sets of system boundaries were used to compute the EROI estimates presented in Table 4 on the corresponding manuscript, including: original EROI estimates from literature without ACP management; revised EROI estimates from literature including ACP treatment in a conventional WWTP from Bauer et al. (2018) [3]; and re-revised EROI estimates from literature accounting for struvite recovery from post-HTL ACP with subsequent conventional treatment in a municipal WWTP to remove TN, TP, and BOD [4–6].. These systems boundaries are illustrated in Figure S2.

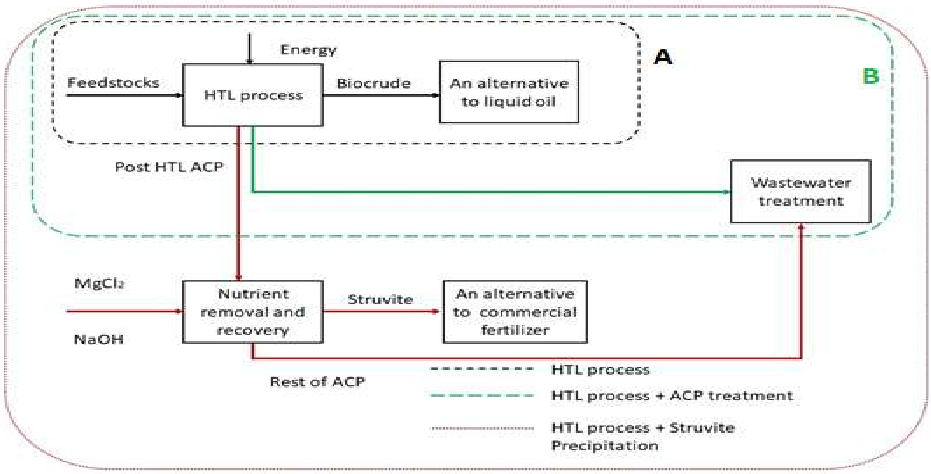

Figure 2. Life cycle boundaries for three estimates of HTL EROI are denoted A, B, and C. "A" (dashed black lines) depicts initial systems boundaries from original HTL studies (i.e., Connelly et al. (2015), Vardon et al. (2012) and Sawayama et al. (1999)). "B" (dashed green lines) depicts revised system boundaries used by Bauer et al. (2018) to account for ACP treatment in a municipal WWTP. "C" (dashed maroon lines) depicts extended system boundaries used in this study to account for struvite recovery followed by conventional treatment to remove residual TN, TP and BOD.

4.0. Confirmation of Experimental Recovery of Struvite via XRD and Chemical Analysis

Experimental precipitation of struvite from post-HTL ACPs from selected organic waste feedstocks was confirmed by X-ray diffraction (XRD) using a Panalytical Empyrean Diffractometer equipped with a Bragg–Bretano HD Prefix module and a GaliPix3D Area Detector operating in scanning line mode. Crystalline solid precipitates were scanned for 2theta = 5 to 70° at a rate of 4 rps and repeated four times in order to improve the signal to noise ratio. Figure S3 summarizes the results of the XRD analysis for standard struvite (using the RRUFF mineral database) [7], red lees, brewing yeast, and spent grains ACP samples. XRD analysis confirms the chemical identity of crystalline struvite for the solids precipitated from red lees, brewing yeast, and spent grains ACP samples. In addition, the comparison of the XRD patterns of standard struvite to that of the struvite recovered from the ACP samples reveals negligible impurities in the precipitates.

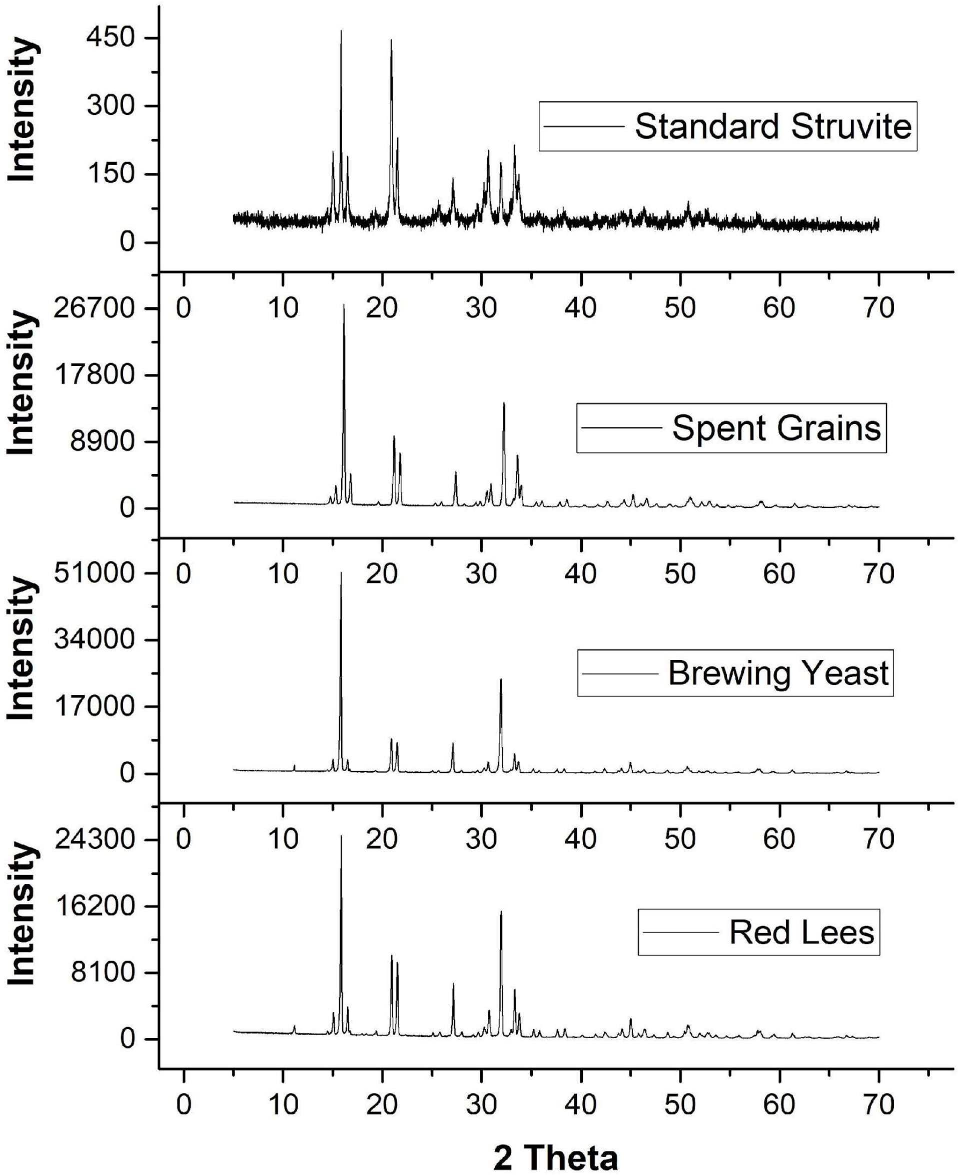

Figure S3. XRD diffractogram of standard struvite and solids precipitated from the post-HTL red lees, brewing yeast and spent grains ACP samples.

Table S9 summarizes the ratio of P–PO_4^{3-}, N–NH_4^+, and Mg^{2+} within the solids precipitated from the post-HTL ACP samples. The molar ratio of P–PO_4^{3-}, N–NH_4^+, and Mg^{2+} as solid precipitates are quite consistent with the average molar ratio of 1.2:1:1.1. The molar ratio of P–PO_4^{3-}, N–NH_4^+, and Mg^{2+} in all solid precipitates is close to 1:1:1, which further confirms the presence of struvite with low impurities.

Table S9. Molar ratio of P–PO_4^{3-}, N–NH_4^+, and Mg^{2+} within the solids precipitated from the post-HTL ACP of select waste feedstocks.

	Molar Ratio of PO_4^{3-}: NH_4^+: Mg^{2+} in Solid Precipitates		
	P–PO_4^{3-}	**N–NH_4^+**	**Mg^{2+}**
Pre-Digested Sludge	1.3	1.0	1.1
Digested Sludge	1.0	1.0	1.1
Brewing Yeast	1.2	1.0	1.0
Spent Grains	1.2	1.0	1.0
White Lees	1.1	1.0	1.1
Red Lees	1.1	1.0	1.1
Average	***1.2***	***1.0***	***1.1***

5.0. Characterization of Post-HTL ACP via Commercial HACH Water Quality Kits

Commercial HACH water quality analysis kits were used to analyze the water quality of the post-HTL ACP samples produced from the HTL conversion of select waste feedstocks. Water quality parameters measured included: total nitrogen (TN), ammonium (N-NH_4^+), total phosphorus (TP), orthophosphate (P-PO_4^{3-}), and magnesium (Mg^{2+}). TN and N-NH_4 were measured using the "High Range Total Nitrogen TNT Persulfate Digestion Method Test" (Method 10072) and the "High Range Ammonia-Nitrogen TNT Salicylate Method Test" (Method 10031), respectively. TP and P-PO_4^{3-} were measured using the "Ultra High Range Phosphorus (Reactive and Total) TNTplus Ascorbic Acid Method Test" (Method 10210). Finally, Mg^{2+} was measured using the "Magnesium TNTplus Vial Method Test" (Method TNT 849). All measurements were completed in triplicate and adjusted based on a developed calibration curve using chemical standards.

6.0. Feedstock Characterization and Biocrude and ACP Yields of Select Waste Feedstocks

Although the main focus of this study is the production and management of post-HTL ACP arising from HTL processing, it is also important to note the composition of raw HTL feedstocks included in this study prior to HTL conversion. Table S10 presents characterization data from the as-received raw waste feedstocks collected for the conversion into liquid biocrude through HTL processing, as adapted from Bauer et al. (2018) [3].

Table S10. Characterization of as-received raw waste feedstocks for processing into liquid biocrude through HTL conversion, as adapted by Bauer et al. (2018).

Waste Feedstock	TSS (wt %)	VS (wt %)	Ash (wt %)	Water Content (wt %)	N (wt %)	C (wt %)
Dairy Manure	15.2 ± 0.8	88.6 ± 1.6	13.0 ± 3.1	84.7 ± 0.8	1.8 ± 0.1	39.8 ± 0.7
Pre-Digested Sludge	10.5 ± 0.5	28.8 ± 0.8	55.7 ± 0.9	89.5 ± 0.5	4.1 ± 0.3	35.2 ± 0.6
Digested Sludge	8.5 ± 1.5	81.9 ± 0.7	32.3 ± 2.2	91.5 ± 1.5	4.4 ± 0.6	24.0 ± 2.1
Brewing Yeast	16.8 ± 0.2	92.9 ± 0.2	7.1 ± 0.2	83.2 ± 0.2	5.3 ± 0.4	44.3 ± 0.3
Spent Grains	22.1 ± 0.8	96.0 ± 1.9	4.0 ± 1.9	77.9 ± 0.8	4.6 ± 0.5	51.7 ± 1.1
White Lees	26.2 ± 0.3	82.0 ± 4.1	18.0 ± 4.1	73.8 ± 0.3	0.38 ± 0.06	41.1 ± 0.9
Red Lees	11.3 ± 0.9	64.2 ± 1.5	35.8 ± 1.5	88.7 ± 0.9	4.1 ± 0.3	42.8 ± 0.9

Though not the main focus of this study, it is also important to note the biocrude and ACP yields arising from the HTL conversion of the select waste feedstocks analyzed in this study. Table S11 presents biocrude and ACP yields from the HTL conversion of select waste feedstocks, as adapted from Bauer et al. (2018) [3].

Table S11. Biocrude and ACP yield from HTL process for select waste feedstocks, as adapted by Bauer et al. (2018).

Waste Feedstock	Biocrude (g)	ACP (g)	ACP:Biocrude
Dairy Manure	10.7	75.4	7
Pre-Digested Sludge	18.7	64.1	3
Digested Sludge	14.5	66	5
Brewing Yeast	6.1	89.5	15
Spent Grains	5.1	76	15
White Lees	10.3	72	7
Red Lees	7.8	78	10
Average	***10.0***	***74.4***	***9.1***

7.0. References

1. Gustafsson, J. P. (2013). Visual MINTEQ Ver. 3.1. KTH, Sweden. Downloaded from <vminteq.lwr.kth.se/>.
2. Clarens, A. F., Resurreccion, E. P., White, M. A. and Colosi, L. M. (2010). Environmental life cycle comparison of algae to other bioenergy feedstocks. *Environ. Sci. Technol.*, 44, 1813-1819.
3. Bauer, S. K., Reynolds, C., Peng, S. and Colosi, L. M. (2018). Evaluating the water quality impacts of hydrothermal liquefaction: Assessment of carbon, nitrogen, and energy recovery impacts. *Bioresource Technology Reports*, 2, 115-120.
4. Connelly, E. B., Colosi, L. M., Clarens, A. F. and Lambert, J. H. (2015). Life cycle assessment of biofuels from algae hydrothermal liquefaction: The upstream and downstream factors affecting regulatory compliance. *Energy & Fuels*, 29, 1653-1661.

5. Vardon, D., Sharma, B., Blazina, G., Rajagopalan, K. and Strathmann, T. (2012). Thermochemical conversion of raw and defatted algal biomass via hydrothermal liquefaction and slow pyrolysis. *Bioresource Technology*, 109, 178-87.
6. Sawayama, S., Minowa, T. and Yokoyama, S.-Y. (1999). Possibility of energy production and CO_2 mitigation by thermochemical liquefaction of microalgae. *Biomass and Bioenergy*, 17, 33-39.
7. Lafuente, B., Downs, R. T., Yang, H. and Stone, N. (2015). The power of databases: The RRUFF project. In: Highlights in Mineralogical Crystallography, T. Armbruster and R. M. Danisi, eds. Berlin, Germany, W. De Gruyter, pp. 1-30.